

# Heavy Fermion Quantum Effects in $SU(2)_L$ Gauge Theory

E. Farhi<sup>a</sup>, N. Graham<sup>b</sup>, R.L. Jaffe<sup>a</sup>, V. Khemani<sup>a</sup>, H. Weigel<sup>1a,c</sup>

<sup>a</sup>Center for Theoretical Physics, Laboratory for Nuclear Science  
and Department of Physics, Massachusetts Institute of Technology  
Cambridge, Massachusetts 02139

<sup>b</sup>Department of Physics, Middlebury College  
Middlebury, VT 05753

<sup>c</sup>Institute for Theoretical Physics, Tübingen University  
D-72076 Tübingen, Germany

MIT-CTP-3350      UNITU-HEP-4/2003

## Abstract

We explore the effects of a heavy fermion doublet in a simplified version of the standard electroweak theory. We integrate out the doublet and compute the exact effective energy functional of spatially varying gauge and Higgs fields. We perform a variational search for a local minimum of the effective energy and do not find evidence for a soliton carrying the quantum numbers of the decoupled fermion doublet. The fermion vacuum polarization energy offsets the gain in binding energy previously argued to be sufficient to stabilize a fermionic soliton. The existence of such a soliton would have been a natural way to maintain anomaly cancellation at the level of the states. We also see that the sphaleron energy is significantly increased due to the quantum corrections of the heavy doublet. We find that when the doublet is slightly heavier than the quantum-corrected sphaleron, its decay is exponentially suppressed owing to a new barrier. This barrier exists only for an intermediate range of fermion masses, and a heavy enough doublet is indeed unstable.

---

<sup>1</sup> Heisenberg Fellow

## I. INTRODUCTION

In a chiral gauge theory like the Standard Model, gauge invariance prevents fermions from having explicit mass terms. Rather, they get their mass through their coupling to a scalar field via the well-known Higgs mechanism. At tree level the fermion obtains a perturbative mass, the product of the corresponding Yukawa coupling and the vacuum expectation value of the scalar Higgs field. The decoupling of such fermions presents interesting unsolved puzzles. Ordinary decoupling arguments [1], which would show that a heavy fermion is irrelevant in the low-energy theory, break down. Increasing the mass, which causes the denominators in the fermion propagators to suppress quantum corrections, also increases the coupling, which gives a corresponding enhancement from the vertices. Furthermore, unlike an ordinary fermion with vector couplings, a chiral fermion cannot simply disappear from the theory as its mass is increased, because anomaly cancellation would be ruined. As shown in ref. [2], gauge invariance is maintained at the level of the Lagrangian because integrating out the heavy fermion induces a Wess-Zumino term in the resulting effective Lagrangian.

For the case of Witten's non-perturbative  $SU(2)$  anomaly [3], one can analyze the theory at the level of the action along the same lines [2]. However, one can also analyze the situation from a different point of view. Ref. [4] shows that this anomaly can be understood in terms of the Hamiltonian of the theory: A theory with an odd number of left-handed fermion doublets has no gauge-invariant states. However, if the Yukawa coupling of a fermion is large enough, the perturbative fermion mass will be larger than the classical energy of the sphaleron [5], so that such fermions are no longer stable states in the spectrum of the theory. Thus, to maintain gauge invariance in the low-energy theory, there must exist either new states in the theory carrying the quantum numbers of the fermion, or a mechanism to suppress the decay of the perturbative fermion states.

Although these scenarios could rely on complicated non-perturbative physics, one simple resolution would be provided by the existence of a soliton carrying the quantum numbers of the decoupled fermion. If a localized configuration of gauge and Higgs fields binds a fermion level tightly, the binding energy could outweigh the cost in classical energy to set up the background field configuration. However, to consistently include the effects of the fermion level, such calculations must also include the Casimir energy, the renormalized shift in the

zero-point energies of all the other fermion modes, since both appear at the same order in  $\hbar$ . For a static field configuration, the Casimir energy represents the full one-loop quantum vacuum polarization energy, equivalent to summing to all orders in the derivative expansion.

To compare the quantum energy of the configuration with the sphaleron, we must also include the corresponding correction to the sphaleron's energy as well. Furthermore, we must check whether the quantum corrections induce an energy barrier between the perturbative fermion and the sphaleron, which would mean that the perturbative fermion would be quasi-stable, only able to decay by tunneling.

We have carried out such calculations in a simplified version of the Standard Model, for background fields in the spherical ansatz, keeping fermion vacuum fluctuations but ignoring those of the gauge and Higgs fields. We find significant quantum corrections to the height of the sphaleron barrier. As we make the fermion level heavier than the quantum corrected sphaleron, we do see evidence for a barrier suppressing its decay. For even larger Yukawa couplings, however, the barrier disappears and the fermion's decay is unsuppressed. We do not see any evidence for a soliton for any value of the Yukawa coupling, and find that including the full Casimir energy destabilizes solitons found in previous work [6].

We comment on possible explanations of this result and its relation to the Witten anomaly in the conclusions.

## II. THE THEORY

We consider the electroweak sector of the Standard Model with three simplifying modifications: (1) the  $U(1)$  hypercharge gauge fields are absent, (2) the fermions within an isospin doublet are degenerate in mass, and (3) the Cabibbo-Kobayashi-Maskawa (CKM) matrix is the identity, so there is no mixing between fermions of different generations. Since there is no  $U(1)$ , the theory does not have any perturbative gauge anomalies, but Witten's non-perturbative anomaly requires it to have an even number of  $SU(2)_L$  fermion doublets.

The Higgs-Gauge sector Lagrangian density is

$$\mathcal{L}_H = -\frac{1}{2}\text{tr}(F^{\mu\nu}F_{\mu\nu}) + \frac{1}{2}\text{tr}\left([D^\mu\Phi]^\dagger D_\mu\Phi\right) - \frac{\lambda}{4}\left[\text{tr}(\Phi^\dagger\Phi) - 2v^2\right]^2, \quad (1)$$

where

$$F_{\mu\nu} = \partial_\mu A_\nu - \partial_\nu A_\mu - ig[A_\mu, A_\nu],$$

$$\begin{aligned}
D_\mu \Phi &= (\partial_\mu - igA_\mu) \Phi, \\
A_\mu &= A_\mu^a \frac{\tau^a}{2},
\end{aligned} \tag{2}$$

and where  $g$  and  $\lambda$  are gauge and Higgs self-interaction coupling constants respectively. Furthermore,  $v$  denotes the tree-level vacuum expectation value of the Higgs field. The  $2 \times 2$  matrix field  $\Phi$  is related to the Higgs doublet  $\phi$  by

$$\Phi = \begin{pmatrix} \phi_2^* & \phi_1 \\ -\phi_1^* & \phi_2 \end{pmatrix}. \tag{3}$$

$\Phi$  can be re-expressed in terms of four real functions as

$$\Phi(x) = v (s(x) + ip^a(x)\tau^a). \tag{4}$$

The fermionic sector Lagrangian density for each isospin doublet is

$$\mathcal{L}_F = \bar{\Psi}_L i\gamma^\mu D_\mu \Psi_L + \bar{\Psi}_R i\gamma^\mu \partial_\mu \Psi_R - f (\bar{\Psi}_L \Phi \Psi_R + \text{h.c.}), \tag{5}$$

where the covariant derivative is the same as in eq. (2) and  $f$  is the Yukawa coupling constant (which may be different for each doublet). There is no coupling between fermions belonging to different isospin doublets owing to our assumption of diagonal CKM matrix. We introduce the potential

$$V(A, \Phi) = -g\gamma^\mu A_\mu(x) \frac{1 - \gamma_5}{2} + f (h(x) + ivp^a(x)\tau^a\gamma_5), \tag{6}$$

where

$$h(x) \equiv v(s(x) - 1), \tag{7}$$

to write this Lagrangian density as the sum of a free part and an interaction part:

$$\mathcal{L}_F = \bar{\Psi} (i\gamma^\mu \partial_\mu - fv) \Psi - \bar{\Psi} V \Psi. \tag{8}$$

We are interested in decoupling a single fermion doublet from the theory and for the remainder of the paper we consider only this single doublet. The full theory is defined by

$$\mathcal{L} = \mathcal{L}_H + \mathcal{L}_F. \tag{9}$$

In the unitary gauge ( $p^a(x) = 0$ ) at tree level, we have a single Higgs particle,  $h(x)$ , with perturbative mass  $m_h^{(0)} = 2v\sqrt{\lambda}$ . The superscript ‘(0)’ denotes that the mass is at tree level. The three gauge fields are degenerate with perturbative mass  $m_w^{(0)} = gv/\sqrt{2}$ . The two degenerate fermions have perturbative mass  $m_f^{(0)} = fv$ .

### III. THE HIGGS-GAUGE SECTOR EFFECTIVE ENERGY

We integrate out the fermion doublet from the theory to obtain the effective action for the Higgs-Gauge sector:

$$e^{iS_{\text{eff}}[A, \Phi]} = e^{i \int d^4x \mathcal{L}_H} \frac{\int [d\Psi][d\bar{\Psi}] e^{i \int d^4x \mathcal{L}_F}}{\int [d\Psi][d\bar{\Psi}] e^{i \int d^4x \mathcal{L}_F|_{V=0}}}. \quad (10)$$

The normalization has been chosen so that the effective action is equal to the classical action for vanishing interaction potential,  $V$ , defined in eq. (6). If  $iS_{\text{FD}}^{(n)}$  denotes the Feynman diagram with one fermion loop and  $n$  external insertions of  $(-iV(A, \Phi))$ , then

$$S_{\text{eff}}[A, \Phi] = \int d^4x \mathcal{L}_H + \sum_{n=1}^{\infty} S_{\text{FD}}^{(n)}. \quad (11)$$

The Feynman diagrams can be computed in a prescribed regularization scheme. The divergences that emerge as the regulator is removed are canceled by counterterms. We introduce the renormalized and counterterm Lagrangians,  $\mathcal{L}_H^{(\text{ren})}$  and  $\mathcal{L}_H^{(\text{ct})}$  respectively, by expressing the bare parameters in  $\mathcal{L}_H$  in terms of renormalized parameters and counterterm coefficients to obtain  $\mathcal{L}_H = \mathcal{L}_H^{(\text{ren})} + \mathcal{L}_H^{(\text{ct})}$ . The renormalized Lagrangian is the original Higgs-Gauge sector Lagrangian, eq. (1), with renormalized parameters substituted and

$$\begin{aligned} \mathcal{L}_H^{(\text{ct})} = & c_1 \text{tr} (F^{\mu\nu} F_{\mu\nu}) + c_2 \text{tr} \left( [D^\mu \Phi]^\dagger D_\mu \Phi \right) \\ & + c_3 [\text{tr} (\Phi^\dagger \Phi) - 2v^2] + c_4 [\text{tr} (\Phi^\dagger \Phi) - 2v^2]^2. \end{aligned} \quad (12)$$

The coefficients  $c_i$  depend on the regulator. For notational simplicity we do not introduce a different notation for the renormalized parameters.

If we consider static Higgs-Gauge fields and restrict time to the interval  $T$ , then the effective energy functional is

$$E_{\text{eff}}[A, \Phi] = - \lim_{T \rightarrow \infty} \frac{1}{T} S_{\text{eff}}[A, \Phi] \equiv E_{\text{cl}}[A, \Phi] + E_{\text{vac}}[A, \Phi], \quad (13)$$

where  $E_{\text{cl}}$  refers to the classical energy of the Higgs-Gauge sector. We use the freedom to make time-dependent gauge transformations to set  $A_0 = 0$ , so that

$$E_{\text{cl}}[A, \Phi] = \int d^3x \left\{ \frac{1}{2} \text{tr} (F_{ij} F_{ij}) + \frac{1}{2} \text{tr} \left( [D_i \Phi]^\dagger D_i \Phi \right) + \frac{\lambda}{4} [\text{tr} (\Phi^\dagger \Phi) - 2v^2]^2 \right\}. \quad (14)$$

The fermionic vacuum polarization energy is

$$E_{\text{vac}}[A, \Phi] = \sum_{n=1}^{\infty} E_{\text{FD}}^{(n)}[A, \Phi] + E_{\text{ct}}[A, \Phi], \quad (15)$$

where each regulated Feynman diagram contribution is

$$E_{\text{FD}}^{(n)}[A, \Phi] = - \lim_{T \rightarrow \infty} \frac{1}{T} S_{\text{FD}}^{(n)}, \quad (16)$$

and the counterterm contribution is

$$E_{\text{ct}}[A, \Phi] = \int d^3x \left\{ -c_1 \text{tr}(F_{ij} F_{ij}) + c_2 \text{tr}([D_i \Phi]^\dagger D_i \Phi) - c_3 [\text{tr}(\Phi^\dagger \Phi) - 2v^2] - c_4 [\text{tr}(\Phi^\dagger \Phi) - 2v^2]^2 \right\}. \quad (17)$$

The entire one-loop effective energy receives contributions also from gauge and Higgs loops. We ignore these contributions because we believe the fermion loops are fundamentally responsible for the phenomena associated with fermion decoupling. If we imagine that the fermions have  $N_C$  internal degrees of freedom (e.g. color), then this approximation becomes exact for large  $N_C$ . Nevertheless we set  $N_C = 1$  in the analysis that follows.

### A. The Counterterms

The counterterms render  $E_{\text{vac}}$  finite by canceling the divergences in  $E_{\text{FD}}^{(n)}$ , for  $n = 1$  through  $n = 4$ , that arise when the regulator is removed. To unambiguously determine the counterterm coefficients,  $c_i$ , we impose conventional renormalization conditions:

- a. We choose the vacuum expectation value (vev) of  $h(x)$  to be 0, which ensures that the vev  $\langle \Phi \rangle = v \mathbb{1}$  stays fixed at its classical value and the perturbative fermion mass does not get renormalized, *i.e.*  $m_f = m_f^{(0)}$ . This is equivalent to a “no-tadpole” renormalization condition and determines  $c_3$ .
- b. We fix the pole of the Higgs propagator to be at the tree level mass,  $m_h = m_h^{(0)}$ , with residue 1. These conditions yield  $c_2$  and  $c_4$ .
- c. We have various choices to fix the remaining undetermined counterterm coefficient  $c_1$ . We choose to set the residue of the pole of the gauge field propagator to 1 in unitary gauge. Then the position of that pole, *i.e.* the mass of the gauge field,  $m_w$ , is a prediction.

The resulting counterterm coefficients,  $c_i$ , are listed in Appendix A. As explained under item c., the mass of gauge fields is constrained by the other model parameters when fermion loops

are included. With our choice of renormalization conditions, it is the solution to the implicit equation

$$m_w^2 = (m_w^{(0)})^2 \left[ 1 + \frac{f^2}{8\pi^2} \left\{ \frac{2}{3} - \frac{m_w^2}{m_f^2} \left( \frac{1}{6} - \int_0^1 dx x^2 (1-x)^2 \frac{m_w^2}{\Delta(x, m_w^2)} \right) + 6 \int_0^1 dx x(1-x) \ln \frac{\Delta(x, m_h^2)}{m_f^2} - \int_0^1 dx \ln \frac{\Delta(x, m_w^2)}{m_f^2} \right\} \right], \quad (18)$$

with  $\Delta(x, q^2) \equiv m_f^2 - x(1-x)q^2$ . Recall that  $m_w^{(0)} = gv/\sqrt{2}$  is the tree level perturbative mass of the gauge fields.

## B. The Vacuum Polarization Energy

We briefly summarize methods introduced in refs. [7, 8] (see ref. [9] for a review and a list of additional references) that enable an *exact* calculation of the fermionic vacuum polarization energy. Eq. (15) gives this energy as an infinite sum of Feynman diagrams. For non-perturbative field configurations all orders would have to be summed, which is intractable. We therefore make use of the fact that it is also given by a sum over the shift in the zero-point energies of the fermion modes due to the background fields. We write this formal quantity as a sum over bound state energies,  $\epsilon_j$ , (times their degeneracies,  $D_j$ ) and a momentum integral of the energy of the continuum states weighted by the change in the density of continuum states,  $\Delta\rho(k)$ , that is induced by the background fields,

$$E_{\text{vac}} = -\frac{1}{2} \sum_j D_j |\epsilon_j| - \frac{1}{2} \int_0^\infty dk \sqrt{k^2 + m_f^2} \Delta\rho(k) + E_{\text{ct}}. \quad (19)$$

The momentum integral and  $E_{\text{ct}}$  are both divergent, but their sum is finite because the theory is renormalizable. We render the integral finite by subtracting the first  $N$  terms in the Born series expansion of the density of states and adding back in exactly the same quantity in the form of Feynman diagrams:

$$E_{\text{vac}} = -\frac{1}{2} \sum_j D_j |\epsilon_j| - \frac{1}{2} \int_0^\infty dk \sqrt{k^2 + m_f^2} \left( \Delta\rho(k) - \sum_{i=1}^N \Delta\rho^{(i)}(k) \right) + \sum_{i=1}^N E_{\text{FD}}^{(i)} + E_{\text{ct}}. \quad (20)$$

When we combine  $E_{\text{ct}}$  with  $\sum_{i=1}^N E_{\text{FD}}^{(i)}$ , we cancel the divergences as well as implement the renormalization prescription. As a result, the above expression is manifestly finite. The

minimal number of required Born subtractions,  $N$ , is easily determined by an analysis of the superficial degree of divergence of the one-loop Feynman diagrams. For our theory,  $N = 4$ .

We will work with background fields in the spherical ansatz [10]. Then we can express  $\Delta\rho(k)$  (and its Born series) in terms of the momentum derivative of the phase shifts [11], induced by the background fields, of the Dirac wave-functions,

$$\Delta\rho(k) = \frac{1}{2\pi i} \frac{d}{dk} \text{Tr} \ln S(k) = \frac{1}{\pi} \frac{d}{dk} \sum_{\sigma \in \{+, -\}} \sum_G D_G \delta_{G,\sigma}(k). \quad (21)$$

Here we have expanded the  $S$ -matrix in grand spin channels labeled by  $G$ . The grand spin is the vector sum of total angular momentum and isospin. It is conserved by the potential, eq. (6). The asymptotic scattering states are labeled by parity  $(-1)^G$  and total spin  $G \pm 1/2$  and we obtain a  $4 \times 4$   $S$ -matrix in general (except in the  $G = 0$  channel, where it is  $2 \times 2$ ). We let  $\delta_{G,\sigma}(k)$  denote the sum of the eigenphase shifts at momentum  $k$  in channel  $G$  and  $\sigma = \pm$  specify the sign of the energy eigenvalue,  $\omega = \pm\sqrt{k^2 + m_f^2}$ . Note that the single particle spectrum is not symmetric because the Dirac Hamiltonian is not charge conjugation invariant. The degeneracy is given by  $D_G = 2G + 1$ . In Appendix B we show in detail how to use the Dirac equation to calculate the bound state energies and scattering phase shifts needed in the computation of  $E_{\text{vac}}$ .

To simplify the calculation we only subtract the first two Born approximants and eliminate the remaining log-divergence in the momentum integral by using a limiting function approach developed in ref. [12]. The final expression for the vacuum polarization energy is

$$E_{\text{vac}} = -\frac{1}{2} \sum_j (2G_j + 1) |\epsilon_j| - \int_0^\infty \frac{dk}{2\pi} \sqrt{k^2 + m_f^2} \frac{d}{dk} \bar{\delta}(k) + E^{(1,2)} + E^{(3,4)}, \quad (22)$$

where  $G_j$  is the grand spin associated with the bound state  $j$  and

$$\bar{\delta}(k) = \sum_{\sigma \in \{+, -\}} \sum_{G=0}^\infty (2G + 1) \left( \delta_{G,\sigma}(k) - \delta_{G,\sigma}^{(1)}(k) - \delta_{G,\sigma}^{(2)}(k) \right) + \delta_{\text{lim}}(k). \quad (23)$$

Here  $\delta_{G,\sigma}^{(i)}(k)$  denotes the  $i^{\text{th}}$ -term in the Born series of  $\delta_{G,\sigma}(k)$ . After subtracting  $\delta^{(1)}$  and  $\delta^{(2)}$  from  $\delta$ , the momentum integral does not contain any contributions that are linear or quadratic in  $V$ . The limiting function for the sum over all eigenphase shifts,  $\delta_{\text{lim}}(k)$ , eliminates the logarithmically divergent pieces that are third and fourth order in  $V$  from the momentum integral. Its analytic expression can be extracted from the divergent pieces of



the corresponding Feynman diagrams and is given in Appendix B, eq. (B18). Furthermore,  $E^{(1,2)}$  denotes the contribution up to second order in  $V$  from the renormalized Feynman diagrams. Its explicit expression is displayed in Appendix B. Finally,  $E^{(3,4)}$  contains the third and fourth order counterterm contribution combined with the divergences in the third and fourth order Feynman diagrams that have been subtracted from the momentum integral via  $\delta_{\text{lim}}$ . Again, its explicit form can be found in Appendix B.

Thus we compute an exact, finite, renormalized, gauge-invariant effective energy functional,  $E_{\text{eff}}[A, \Phi]$ , defined in eq. (13), for the Higgs-Gauge sector, with the fermion fields integrated out.

#### IV. THE ENERGY OF A FERMIONIC CONFIGURATION

We are interested in exploring the possibility of the emergence of a stable, fermionic soliton in the Higgs-Gauge sector of the theory as we increase the Yukawa coupling (thereby making the perturbative fermion heavier). In the previous section we outlined the procedure that allows us to calculate the effective energy when the fermions are integrated out. Now we analyze the minimum additional energy required to associate unit fermion number with a particular Higgs-Gauge configuration  $C$ , where  $C \equiv \{A, \Phi\}$ . First in section IV A we determine the integer fermion number  $F[C]$  of a configuration. (This is subtle because we have to contend with the anomalous violation of fermion number). Then we occupy or empty levels of the single-particle Dirac Hamiltonian to obtain the lowest energy state with net fermion number 1. If  $F[C] = 0$ , then the lightest positive bound state needs to be filled and the occupation energy  $E_{\text{occ}}^{(1)} = \epsilon_{\text{lowest}}$ , where the superscript ‘(1)’ denotes that levels have been occupied/emptied to obtain fermion number 1. If  $F[C] = 1$  then  $E_{\text{occ}}^{(1)} = 0$  because  $C$  is already fermionic, and so on. Thus, the minimum total energy of a single fermion associated with a configuration is

$$E_{\text{eff}}^{(1)}[C] = E_{\text{cl}}[C] + E_{\text{vac}}[C] + E_{\text{occ}}^{(1)}[C]. \quad (24)$$

In previous works, such as [6], the vacuum polarization contribution was omitted from the above equation and stable non-topological solitons were found. We consider such calculations inconsistent, because  $E_{\text{occ}}^{(1)}$  and  $E_{\text{vac}}$  are both order  $\hbar$ . We will see explicitly in section V C that  $E_{\text{vac}}$  makes a significant positive contribution when the Yukawa coupling is large enough

that the perturbative fermion mass is comparable to the classical energy.

Since we refer to all these different energies frequently in the rest of the paper, we summarize our notation in Table I.

$E_{\text{cl}}$	Classical Higgs and gauge energy, eq. (14)
$E_{\text{vac}}$	Fermion vacuum polarization energy, including counterterms, eqs. (15, 19)
$E_{\text{eff}}$	One-fermion-loop effective energy, $E_{\text{cl}} + E_{\text{vac}}$
$E_{\text{occ}}^{(m)}$	Smallest occupation energy required to obtain fermion number $m$ , eq. (24)
$E_{\text{eff}}^{(m)}$	Smallest effective energy in the fermion number $m$ sector, $E_{\text{eff}} + E_{\text{occ}}^{(m)}$

TABLE I: Definitions of some of the energies which appear in our analysis.

### A. The Fermion Number of a Configuration

First we review properties of the Higgs-Gauge configuration space and the classical energy functional defined on it. From the expression for  $E_{\text{cl}}$  in eq. (14), it follows that configurations

$$A_j = \frac{i}{g} U^{(n)} \partial_j U^{(n)\dagger}, \quad \Phi = vU^{(n)}, \quad (25)$$

have  $E_{\text{cl}} = 0$  and we refer to them as *zero-classical-energy configurations*. Here  $U^{(n)}$  is any map from  $S^3$  to  $SU(2)$  with winding number  $n$ . Zero-classical-energy configurations with the same winding number are equivalent under small (winding number 0) gauge transformations. We use  $\mathcal{C}^{(n)}$  to denote the homotopic class of zero-classical-energy configurations with winding number  $n$ . Topologically inequivalent zero-classical-energy configurations are related by large (nonzero winding number) gauge transformations. Along any continuous interpolation between two configurations, one in  $\mathcal{C}^{(n)}$  and the other in  $\mathcal{C}^{(m)}$  (with  $n \neq m$ ), there exists a configuration,  $C$ , with maximum classical energy. Since no  $U^{(n)}$  can be continuously deformed into any  $U^{(m)}$ ,  $E_{\text{cl}}[C] > 0$ . The configuration corresponding to the minimax of these energies, when all interpolations are considered, is the *classical sphaleron*. When the fermion vacuum polarization energy is added to the classical energy to obtain the effective energy ( $E_{\text{eff}} = E_{\text{cl}} + E_{\text{vac}}$ ), not only does the magnitude of the minimax energy change, but its location in configuration space shifts as well. We therefore define the *quantum-corrected*

*sphaleron* to be the configuration that has the lowest of the maximum effective energies along all interpolations between topologically inequivalent zero-classical-energy configurations.

We associate any configuration  $C$  with a unique class of zero-classical-energy configurations by continuously deforming  $C$  in the direction of the negative gradient of the classical energy until we get a configuration in  $\mathcal{C}^{(n)}$  for some  $n = n(C)$ . We call  $\mathcal{C}^{(n(C))}$  the *connected  $\mathcal{C}$ -class* of  $C$  and we say that  $C$  is in the winding number  $n$  basin. Note that the classical sphaleron and all configurations that descend to it are on the boundary between different basins.

For any two configurations  $C_1$  and  $C_2$ , we define the *spectral flow*  $S[C_1, C_2]$  to be the number of eigenvalues (levels) of the single particle Dirac Hamiltonian that cross zero from above minus the number that cross zero from below along any interpolation from  $C_1$  to  $C_2$ . The fermion number of a configuration  $C$  is defined as

$$F[C] = S[C_1, C] \tag{26}$$

with  $C_1 \in \mathcal{C}^{(n(C))}$ . Since the Dirac spectrum is gauge-invariant,  $F[C]$  does not depend on which particular  $C_1$  is chosen from the connected  $\mathcal{C}$ -class. Moreover,  $F[C]$  is gauge-invariant even under large gauge transformations. Also,  $F[C]$  does not depend on the chosen interpolation because the spectral flow is the same for all interpolations. This definition of the fermion number can be readily understood for a  $C$  that has classical energy less than the energy of the classical sphaleron. A continuous interpolation from any configuration in  $\mathcal{C}^{(n(C))}$  to  $C$  preserves net fermion number because anomalous fermion number violations require the Higgs-Gauge fields to cross the sphaleron barrier. Thus, defining zero-classical-energy configurations to have zero fermion number leads to eq. (26). Configurations that have classical energies larger than the classical sphaleron are not separated by an energy barrier from topologically inequivalent basins, so it is not clear what their fermion number should be, although our definition does assign a unique  $F$  to them.

Having determined the fermion number of a configuration, we can use eq. (24) to find  $E_{\text{eff}}^{(1)}$ , the minimum effective energy of a configuration in the fermion number 1 sector.

## B. Stability of the Soliton

We would like to know if there exists a configuration at which the one-fermion effective energy functional,  $E_{\text{eff}}^{(1)}$ , has a local minimum. This configuration would be a fermionic soliton. We carry out a variational search, looking for a configuration  $C$  such that  $E_{\text{eff}}^{(1)}[C] < m_f$  and  $E_{\text{eff}}^{(1)}[C] < E_{\text{q.s.}}$ , where  $E_{\text{q.s.}}$  is the effective energy of the quantum-corrected sphaleron. The first condition ensures that  $C$  cannot simply decay into a configuration with zero classical energy plus a perturbative fermion. The second condition prevents  $C$  from rolling over the quantum-corrected sphaleron, giving up its fermion number and then rolling down the  $E_{\text{eff}}^{(0)}$  surface to a zero-classical-energy configuration. Finding a configuration with these properties would guarantee the existence of a nontrivial local minimum of  $E_{\text{eff}}^{(1)}$ .

## V. THE SEARCH FOR THE SOLITON

In this section we describe our search for the soliton. We first review the spherical ansatz for the gauge and Higgs fields. We then outline the restrictions imposed on the variational ansätze used to search for a soliton. Finally, we report on our search within two physically motivated sets of ansätze: the “twisted Higgs” and “paths over the sphaleron”. Note that throughout this section the perturbative fermion mass is set to 1 so that energies and lengths are measured in units of  $m_f$  and  $1/m_f$ , respectively.

### A. The Spherical Ansatz

We only consider static gauge and Higgs fields in the spherical ansatz. This enables us to expand the fermion S matrix in terms of partial waves labeled by the grand spin  $G$ , as described in Appendix B. Our method for calculating the fermion vacuum polarization energy requires such an expansion. Under these restrictions (and in the  $A_0 = 0$  gauge, which for smooth fields is obtained by a non-singular gauge transformation), the fields can be expressed in terms of five real functions of  $r$ :

$$\begin{aligned} A_i(\vec{x}) &= -A^i(\vec{x}) = \frac{1}{2g} \left[ a_1(r) \tau_j \hat{x}_j \hat{x}_i + \frac{\alpha(r)}{r} (\tau_i - \tau_j \hat{x}_j \hat{x}_i) + \frac{\gamma(r)}{r} \epsilon_{ijk} \hat{x}_j \tau_k \right], \\ \Phi(\vec{x}) &= v [s(r) + ip(r) \tau_j \hat{x}_j], \end{aligned} \tag{27}$$

where  $\hat{x}$  is the unit three-vector in the radial direction.

The ansatz transforms under a  $U(1)$  subgroup of the full  $SU(2)$  gauge symmetry, corresponding to elements of the form

$$g(\vec{x}) = e^{if(r)\tau_j \hat{x}_j/2}, \quad (28)$$

with  $a_1$  transforming as a 1 dimensional vector field,  $s + ip$  as a scalar with charge  $1/2$ , and  $\alpha + i(\gamma - 1)$  as a scalar with charge 1. It is thus convenient to introduce the moduli  $\rho, \Sigma$  and phases  $\theta, \eta$  for the charged scalars:

$$-i\rho e^{i\theta} \equiv \alpha + i(\gamma - 1) \quad \text{and} \quad \Sigma e^{i\eta} \equiv s + ip. \quad (29)$$

From now on we will specify a configuration using the five functions  $a_1(r), \rho(r), \theta(r), \Sigma(r)$  and  $\eta(r)$ . Regularity of  $A_i(\vec{x})$  and  $\Phi(\vec{x})$  at  $\vec{x} = 0$  requires that

$$\begin{aligned} \rho(0) &= 1, \\ \rho'(0) &= 0, \\ \theta(0) &= -2n_\theta\pi, \\ a_1(0) &= \theta'(0), \\ \text{either } \Sigma(0) &= 0 \text{ or } \eta(0) = -n_\eta\pi. \end{aligned} \quad (30)$$

Here  $n_\theta, n_\eta$  are integers and primes denote derivatives with respect to the radial coordinate.

For the gauge transformation  $g(\vec{x})$  in eq. (28) to be non-singular, we require  $f(0) = -2n\pi$ , where  $n$  is an integer and we denote this boundary condition as a superscript:  $f(r) \equiv f^{(n)}(r)$ . If  $f^{(n)}(r)$  is restricted to be 0 as  $r \rightarrow \infty$  (which is equivalent to  $g(r \rightarrow \infty) = \mathbb{1}$ ) then  $n$  is the winding of the map  $g(\vec{x}) : S^3 \rightarrow SU(2)$ . So the topology of the zero-classical-energy configurations persists in the spherical ansatz. The classical energy of eq. (14) takes the form

$$\begin{aligned} E_{\text{cl}} = 4\pi \int_0^\infty dr \left\{ \frac{1}{g^2} \left[ \rho'^2 + \rho^2(\theta' - a_1)^2 + \frac{(\rho^2 - 1)^2}{2r^2} \right] \right. \\ \left. + \frac{1}{f^2} \left[ r^2 \Sigma'^2 + r^2 \Sigma^2 (\eta' - \frac{1}{2}a_1)^2 + \frac{r^2}{4} m_h^2 (\Sigma^2 - 1)^2 \right. \right. \\ \left. \left. + \frac{1}{2} \Sigma^2 \left( (\rho - 1)^2 + 4\rho^2 \sin^2 \frac{\theta - 2\eta}{2} \right) \right] \right\}, \end{aligned} \quad (31)$$

and winding number  $n$  zero-classical-energy configurations of eq. (25) now become

$$\begin{aligned} \rho(r) &= 1, \quad \Sigma(r) = 1, \\ \theta(r) &= f^{(n)}(r), \quad \eta(r) = \frac{f^{(n)}(r)}{2}, \quad a_1(r) = f^{(n)'}(r). \end{aligned} \quad (32)$$

We want the Higgs-Gauge fields to have finite classical energy. So we require a field configuration of the form eq. (32) as  $r \rightarrow \infty$ , and the restriction that  $f^{(n)}(\infty) = 0$  uniquely specifies the boundary conditions on the fields at infinity. At  $\vec{x} = 0$ , the boundary conditions on  $\rho$  (specified in eq. (30)) make the energy density finite and we do not require any additional constraints.

The anomalous violation of fermion number is given by the anomaly equation

$$\partial_\mu (\bar{\Psi} \gamma^\mu \Psi) = \partial_\mu K^\mu, \quad (33)$$

where  $K^\mu$  is the Chern-Simons current. It is useful to consider the charge associated with it:

$$\begin{aligned} N_{\text{CS}} &= -\frac{g^2}{8\pi^2} \epsilon_{ijk} \int d^3x \text{tr} \left( A_i \partial_j A_k - \frac{2}{3} ig A_i A_j A_k \right) \\ &= \frac{1}{2\pi} \int_0^\infty dr [a_1 + \rho^2(\theta' - a_1)]. \end{aligned} \quad (34)$$

This is a non-integer in general, and is equal to the integer winding number of  $f^{(n)}$  for the configurations of eq. (32), and a half-integer for the sphaleron [13]. Under a winding  $n$  gauge transformation,  $N_{\text{CS}} \rightarrow N_{\text{CS}} + n$ . For background fields that interpolate between topologically distinct zero-classical-energy configurations, the net fermion number produced is given by the change in  $N_{\text{CS}}$ .

## B. Restrictions on the Variational Ansätze

Our methods allow us to consider any static, spherically symmetric configuration,  $C$ , in the Higgs-Gauge sector, specified by the five real functions  $a_1(r)$ ,  $\rho(r)$ ,  $\theta(r)$ ,  $\Sigma(r)$  and  $\eta(r)$ . In principle, we could numerically minimize the fermionic energy,  $E_{\text{eff}}^{(1)}[C]$ , in terms of the five functions and determine if a soliton exists. In practice however, that is not feasible. So instead we limit ourselves to the variation of a few parameters in ansätze motivated by physical considerations.

We restrict our variational ansätze to those that obey the above described boundary conditions at the origin and at infinity. In addition, we restrict the Higgs fields to lie within the chiral circle,  $\Sigma(r) < 1$ , because otherwise the effective potential is unbounded from below. (The leading terms in the derivative expansion of eq (10) can be found in [14]). Finally, the effective theory (obtained by integrating out the fermions) has a Landau pole

in the ultraviolet, reflecting new dynamics at some cutoff energy scale or equivalently at a minimum distance scale. Configurations that are large compared to this distance scale are relatively insensitive to the new dynamics at the cutoff, but smaller configurations are sensitive. For small widths and large couplings, the Landau pole becomes significant and leads to unphysical negative effective energies in eq. (13) [15]. We have to be wary of this in estimating the reliability of our results. See [12] for more detailed discussions on the effective potential and the Landau pole.

### C. Twisted Higgs

We first consider twisted Higgs configurations, with  $n_\eta = 1$  so that  $\eta(r)$  goes from  $-\pi$  at  $r = 0$  to 0 as  $r \rightarrow \infty$ . The other functions are trivial:  $a_1(r) = 0, \rho(r) = 1, \theta(r) = 0$  and  $\Sigma(r) = 1$ . If we smoothly interpolate from a zero-classical-energy configuration (in the connected  $\mathcal{C}$ -class) to such a configuration, we observe that one fermion bound state, that originates in the positive continuum, has its energy decrease sharply. The wider the final twisted Higgs configuration, the closer this level ends up to the negative continuum. At a width of order  $1/m_f$ , it has energy zero, eliminating any occupation energy contribution,  $E_{\text{occ}}^{(1)}$ , to the fermionic energy,  $E_{\text{eff}}^{(1)}$ , associated with it. The existence of this level makes such twisted Higgs configurations attractive candidates for the variational search.

We consider one such twisted Higgs configuration with a width characterized by a variational parameter  $w$ ,

$$\eta = -\pi e^{-r/w} \quad (35)$$

and add various perturbations to it. For instance, one among many of our variational ansätze (in the  $\theta = 0$  gauge) is a four parameter ansatz with parameters  $p_0, \dots, p_3$ :

$$\begin{aligned} \eta &= -\pi e^{-r/w} + p_0 \frac{r/w}{1 + (r/w)^2} e^{-r/w}, \\ \Sigma &= 1 + p_1 \frac{1}{1 + (r/w)} e^{-r/w}, \\ a_1 &= p_2 \frac{r/w}{1 + (r/w)^2} e^{-r/w}, \\ \rho &= 1 + p_3 \frac{(r/w)^2}{1 + (r/w)^3} e^{-r/w}, \end{aligned} \quad (36)$$

where  $-1 < p_1 < 0$  (to keep the Higgs field within the chiral circle and its magnitude positive) and  $p_3 > -5.23$  (to keep  $\rho$  positive). For a prescribed set of theory parameters

( $m_w, m_h$  and  $f$ ) we determine the gauge coupling  $g = \sqrt{2}m_w^{(0)}/v$  from the renormalization constraint eq. (18). We then vary the ansatz parameters ( $w, p_0, \dots, p_3$ ) to lower the fermionic energy  $E_{\text{eff}}^{(1)}$ . We find that the gain in binding energy is insufficient to compensate for the increase in the effective energy  $E_{\text{eff}}$ . Through all our variations,  $E_{\text{eff}}^{(1)}$  is strictly greater than  $m_f$  and we find no evidence for a soliton. The same result was obtained in [12] without gauge fields, and the extra gauge degrees of freedom do not seem to help in the twisted Higgs ansatz.

We find that the fermion vacuum polarization contribution,  $E_{\text{vac}}$ , to the fermionic energy,  $E_{\text{eff}}^{(1)}$  destabilizes would-be solitons. Consider a linear interpolation from the trivial zero-classical-energy configuration to the twisted Higgs configuration in eq. (35) with gauge fields set to zero. We introduce the interpolating parameter  $\xi$  which goes from 0 to 1:

$$\Sigma e^{i\eta} = 1 - \xi + \xi \exp(-i\pi e^{-r/w}). \quad (37)$$

We choose the Yukawa coupling to be  $f = 10$  and the Higgs mass to be  $v/\sqrt{2}$ . Since the gauge fields are trivial, the classical energy as well as the Dirac spectrum are independent of the gauge coupling  $g$  and the gauge bosons mass  $m_w$ . For each value of  $\xi$ , we compute  $E_{\text{eff}}^{(1)}$  and  $E_{\text{eff}}^{(1)} - E_{\text{vac}}$  for different values of the width parameter  $w$ . In Fig. 1 we plot  $E_{\text{eff}}^{(1)}$  and  $E_{\text{eff}}^{(1)} - E_{\text{vac}}$  as functions of  $\xi$ , choosing the width at every point to minimize the energy (we do not allow  $w$  to be less than 1 so that we remain relatively insensitive to the Landau pole). For all points on the plot there is no spectral flow and so  $E_{\text{eff}}^{(1)} = E_{\text{cl}} + \epsilon_{\text{lowest}} + E_{\text{vac}}$  in accordance with eq. (24), where  $\epsilon_{\text{lowest}}$  is the smallest positive bound-state energy in the Dirac spectrum. If  $E_{\text{vac}}$  is omitted, for  $0 < p < 0.6$  we have configurations that have fermionic energies lower than the mass of the perturbative fermion ( $m_f = 1$  in our units). These configurations indicate the existence of a local minimum on the  $E_{\text{eff}}^{(1)} - E_{\text{vac}}$  surface which would be a soliton. The  $E_{\text{vac}}$  contribution, however, raises the energies of the configurations to above  $m_f$  as shown in the figure, and the would-be solitons are destabilized.

#### D. Paths over the Sphaleron

The gauge fields introduce another mechanism for strongly binding a fermion state: there is a zero mode in the background of the sphaleron. Along an interpolation of the background fields from a configuration in  $\mathcal{C}^{(n)}$  to a configuration in  $\mathcal{C}^{(n+1)}$ , a fermion level leaves the



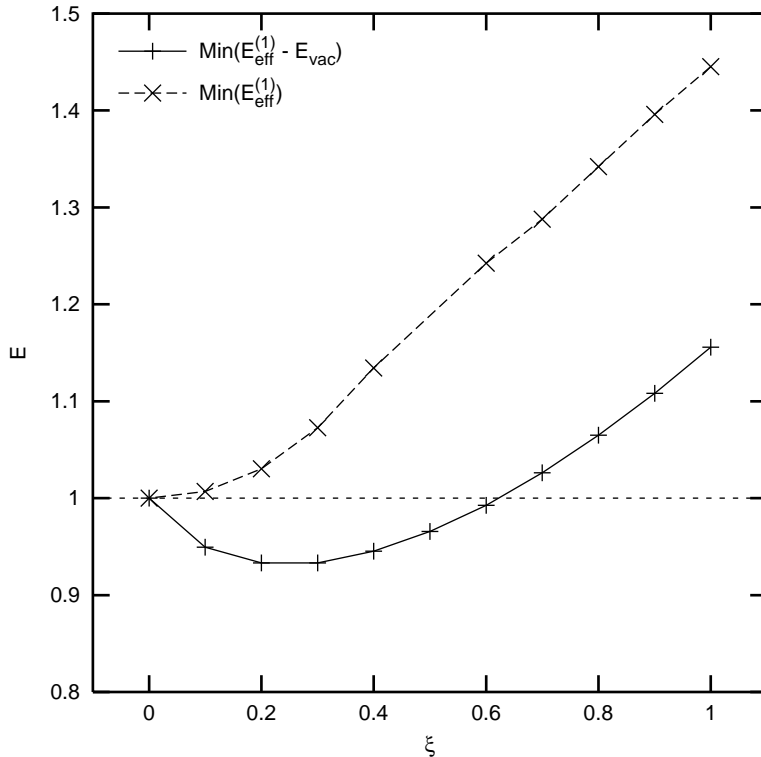


FIG. 1: Minimum fermionic effective energies (in units of  $m_f$ ), with as well as without  $E_{\text{vac}}$  contributions, along the interpolation in eq. (37).

positive continuum, crosses zero from above and finally enters the negative continuum. The lowering of the occupation energy,  $E_{\text{occ}}^{(1)}$ , as we approach zero from above is offset by the rising effective energy ( $E_{\text{eff}} = E_{\text{cl}} + E_{\text{vac}}$ ), so we must investigate whether the former can dominate the latter. We also use such interpolations to study the effects of a large Yukawa coupling on the sphaleron. We approximate the quantum-corrected sphaleron by minimizing the effective energy barrier between topologically inequivalent zero-classical-energy configurations, with respect to the variational parameters of our interpolations. We also investigate the possible emergence of new barriers in the one-fermion energy surface when the perturbative fermion becomes heavier than the quantum-corrected sphaleron. These last two phenomena affect the stability of the heavy fermion and in some models may be significant for baryogenesis.

We make the following choices for the theory parameters: we fix the Yukawa coupling at  $f = 10$ , which is large enough that fermion effects are significant, but small enough to prevent our configurations from being affected by the Landau pole. Indeed we encounter no negative energy instabilities in our computations of  $E_{\text{vac}}$  for this coupling. We keep the

Higgs mass fixed at  $v/\sqrt{2}$ , which corresponds to  $m_h = \frac{m_f}{\sqrt{2}f} \approx 0.07m_f$ . We choose  $g$  to keep the quantum-corrected sphaleron energy comparable to  $m_f$ , since it is plausible that the mass of the sphaleron sets the scale for decoupling. If the sphaleron is too heavy compared to the fermion, the binding energy gained by the level crossing would be washed out by the effective energy of the sphaleron. For  $g = 6.5$  our best approximation to the quantum-corrected sphaleron is approximately degenerate with the fermion. When the gauge coupling is given, the mass  $m_w$  of the gauge boson is determined from the renormalization constraint eq. (18):  $m_w \approx 0.63m_f$  for  $g = 6.5$  and  $m_w \approx 0.98m_f$  for  $g = 10$ . These theory parameters are of course large deviations from the Standard Model parameters. We exaggerate them to see the effects of the heavy perturbative fermion. Another concern is that for large  $g$ , we should consider quantum fluctuations of the Higgs-Gauge fields. However, we believe that anomaly cancellation drives the creation of a soliton, which would suggest that the fermion vacuum polarization contains the essential physics, and our methods allow us to exactly compute this contribution to the energy for any Yukawa coupling.

First we consider a linear interpolation between a winding-0 and a winding-1 zero-classical-energy configuration. The interpolation parameter  $\xi$  goes from 0 to 1:

$$\begin{aligned}\Phi &= v(1 - \xi)\mathbf{1} + \xi v U^{(1)}, \\ A_j &= \xi \frac{i}{g} U^{(1)} \partial_j U^{(1)\dagger}.\end{aligned}\tag{38}$$

In the spherical ansatz,  $U^{(1)}(\vec{x}) = g(\vec{x})$  is specified by a single function, as in eq. (28), that we choose to be

$$f^{(1)}(r) = -2\pi e^{-r/w},\tag{39}$$

where  $w$  characterizes the width of the configuration. We interpolate  $\xi$  from 0 (the trivial configuration with  $N_{\text{CS}} = 0$ ) to 1/2 (a configuration with  $N_{\text{CS}} = 1/2$  in the presence of which the fermion has a zero mode) and vary  $w$  along the interpolation to minimize  $E_{\text{eff}}^{(1)}$ . This gives an upper bound on the minimum  $E_{\text{eff}}^{(1)}$  as a function of  $N_{\text{CS}}$ . For  $N_{\text{CS}} = 1/2$ , this is an upper bound on the quantum-corrected sphaleron energy as well, because  $E_{\text{eff}}^{(1)} = E_{\text{eff}}$  in the presence of a fermion zero mode (the occupation energy is then 0)<sup>2</sup>. An exploration of  $N_{\text{CS}}$

---

<sup>2</sup> Our numerical methods do not allow us to consider  $N_{\text{CS}}$  exactly equal to 1/2, because the Higgs magnitude vanishes at  $r = 0$  and the second order Dirac equations develop a singularity (as discussed in Appendix B), but we can compute  $E_{\text{eff}}^{(1)}$  very close to  $N_{\text{CS}} = 1/2$ .

between 0 and 1/2 is sufficient to map to all values of  $N_{\text{CS}}$ , since configurations with  $N_{\text{CS}}$  between 1/2 and 1 are obtained by charge conjugation, and configurations with  $N_{\text{CS}} < 0$  or  $N_{\text{CS}} > 1$  are large-gauge-equivalent to configurations with  $N_{\text{CS}}$  between 0 and 1.

We also consider an instanton-like configuration where the Euclidean time  $\xi = x_4$  is the interpolation parameter (which varies from  $-\infty$  to  $\infty$ ) between two topologically inequivalent zero-classical-energy configurations:

$$\begin{aligned} A_\mu &= h(r, \xi) \frac{i}{g} U_{\text{inst}}(\vec{x}, \xi) \partial_\mu U_{\text{inst}}^\dagger(\vec{x}, \xi), \\ \Phi &= v \sqrt{h(r, \xi)} U_{\text{inst}}(\vec{x}, \xi), \end{aligned} \quad (40)$$

where

$$U_{\text{inst}}(\vec{x}, \xi) = \frac{\xi + i\tau_j x_j}{\sqrt{r^2 + \xi^2}} \quad (41)$$

is the canonical winding-1 map from  $S^3$  (space-time infinity) to  $SU(2)$ . Furthermore  $h$  is a function of the Euclidean space-time radius ( $\sqrt{r^2 + \xi^2}$ ) and goes from 0 to 1 as this radius goes from 0 to  $\infty$ . 't Hooft's electroweak instanton [16] is constructed as a self-dual gauge field configuration in the topological charge one sector, and a Higgs field configuration that minimize the covariant kinetic term in the Lagrangian density. This gives

$$h(r, \xi) = \frac{r^2 + \xi^2}{r^2 + \xi^2 + w^2} \quad (42)$$

for any width  $w$  (the classical theory with no Higgs field is scale-invariant). We modify this radial function to exponentially approach its asymptotic value of 1, so that the potential in our Dirac equation falls off fast enough to have a well-defined scattering problem (as described in Appendix B). We choose

$$h(r, \xi) = 1 - e^{-(r^2 + \xi^2)/w^2}. \quad (43)$$

This choice does not minimize any part of the classical Euclidean action (in the topological charge one sector). Since we are interested in minimizing  $E_{\text{eff}}^{(1)}$ , which has fermion vacuum energy and occupation energy contributions in addition to the Higgs-Gauge sector classical energy, we do not need our configurations to minimize the classical energy. In fact, as we describe later, the configurations that minimize  $E_{\text{eff}}^{(1)}$  are rather different from those that minimize  $E_{\text{cl}}$ .

In order to compute the Dirac spectrum for this background using the methods described in Appendix B, we gauge transform to  $A_0 = 0$  and  $\lim_{r \rightarrow \infty} \eta = \lim_{r \rightarrow \infty} \theta = 0$  using the

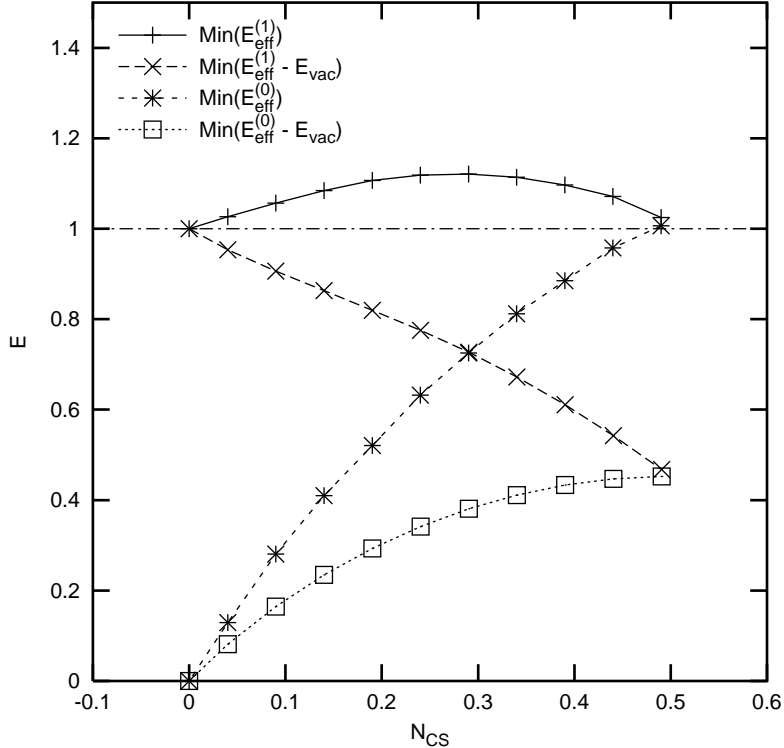


FIG. 2: Minimum effective energies (in units of  $m_f$ ) along the linear path in eqs. (38, 39), in both the zero-fermion and one-fermion sectors (with as well as without the  $E_{\text{vac}}$  contributions).

transformation function

$$f(r, \xi) = \int_{-\infty}^{\xi} d\xi' \frac{2r}{r^2 + (\xi')^2} h(r, \xi') - 2\pi \quad (44)$$

in eq. (28). Finally, as in the case of the linear interpolation, we consider  $\xi$  from  $-\infty$  (the trivial configuration with  $N_{\text{CS}} = 0$ ) to 0 (a configuration with  $N_{\text{CS}} = 1/2$  in the presence of which the fermion has a zero mode) and for each  $\xi$  we choose the  $w$  that minimizes  $E_{\text{eff}}^{(1)}$ .

In Fig. 2 we plot the minimum effective energies in both the zero-fermion sector ( $E_{\text{eff}}^{(0)}$ ) and the one-fermion sector ( $E_{\text{eff}}^{(1)}$ ), minimized within our variational ansatz for the linear interpolation, as functions of the Chern-Simons number,  $N_{\text{CS}}$  (see eqs. (38,39)). As mentioned before, we fix the theory parameters at a Yukawa coupling of  $f = 10$ , a gauge coupling of  $g = 6.5$  and a Higgs mass of  $m_h \approx 0.07m_f$ . These parameters determine the mass of the gauge bosons to be  $m_w \approx 0.63m_f$  from the renormalization constraint, eq. (18). To isolate and highlight the contribution of the fermion vacuum polarization energy,  $E_{\text{vac}}$ , we also plot the energies minimized with  $E_{\text{vac}}$  subtracted.

First consider the zero-fermion sector with the two curves  $E_{\text{eff}}^{(0)}$  and  $E_{\text{eff}}^{(0)} - E_{\text{vac}}$ . For

all points on the plot there is no spectral flow and so  $E_{\text{eff}}^{(0)} - E_{\text{vac}} = E_{\text{cl}}$ . At  $N_{\text{CS}} = 0$ , both  $E_{\text{eff}}^{(0)}$  and  $E_{\text{cl}}$  are minimized at the trivial zero-classical-energy configuration, eq. (32) with  $f^{(0)}(r) = 0$ . At  $N_{\text{CS}} = 1/2$ ,  $E_{\text{eff}}^{(0)}$  is minimized at the quantum-corrected sphaleron while  $E_{\text{cl}}$  is minimized at the classical sphaleron. Within our variational ansatz, we find the parameters that minimize  $E_{\text{eff}}^{(0)}$  at  $N_{\text{CS}} = 1/2$  are different from those that minimize  $E_{\text{cl}}$ . So our approximation to the quantum-corrected sphaleron is distinct from our approximation to the classical sphaleron. Moreover, the fermion vacuum polarization energy correction to the sphaleron turns out to be rather large. Our classical sphaleron has an energy of  $0.45m_f$  (which agrees well with the numerical estimate of  $E = 1.52 \frac{4\pi v \sqrt{2}}{g}$  in [13]), while our quantum-corrected sphaleron has an energy of  $1.02m_f$ .

Next consider the  $E_{\text{eff}}^{(1)}$  and  $E_{\text{eff}}^{(1)} - E_{\text{vac}}$  plots in the one-fermion sector in Fig. 2. Again, for all points on the plot there is no spectral flow and so  $E_{\text{eff}}^{(1)} = E_{\text{cl}} + \epsilon_{\text{lowest}} + E_{\text{vac}}$  in accordance with eq. (24), where  $\epsilon_{\text{lowest}}$  is the smallest positive bound-state energy in the Dirac spectrum. Since the classical sphaleron has an energy much smaller than the perturbative fermion mass, one would expect that the perturbative fermion would have an unsuppressed decay mode over the sphaleron, as first pointed out by Rubakov in [17]. The  $E_{\text{eff}}^{(1)} - E_{\text{vac}}$  curve indeed displays this decay path. The fermion vacuum polarization energy modifies things in two crucial ways. First, the fermion quantum corrections to the sphaleron raise its energy to be degenerate with the fermion, as mentioned before. So the threshold mass is significantly increased. Second, in the plot of  $E_{\text{eff}}^{(1)}$  we observe that there is an energy barrier between the fundamental fermion and the quantum-corrected sphaleron. This indicates that even when the fermion becomes heavier than the sphaleron, there might exist a range of masses for which the decay continues to be exponentially suppressed (since it can proceed only via tunneling).

In Fig. 3 we restrict our attention to the one-fermion sector and consider the linear interpolation and the instanton-like interpolation. In addition to  $g = 6.5$  we consider  $g = 10$ , which corresponds to  $m_w \approx 0.98m_f$ . For each of these two gauge couplings, we plot the effective energy minimized within our ansätze as a function of  $N_{\text{CS}}$  for the two interpolations.

The two seemingly different interpolating configurations produce very similar minimum  $E_{\text{eff}}^{(1)}$  curves. Furthermore, when we enlarge the variational ansätze in our interpolations, we are unable to reduce the energies by any significant amount. Thus we speculate that the plotted curves may be close to tight upper bounds on the true minimum  $E_{\text{eff}}^{(1)}$  curve.

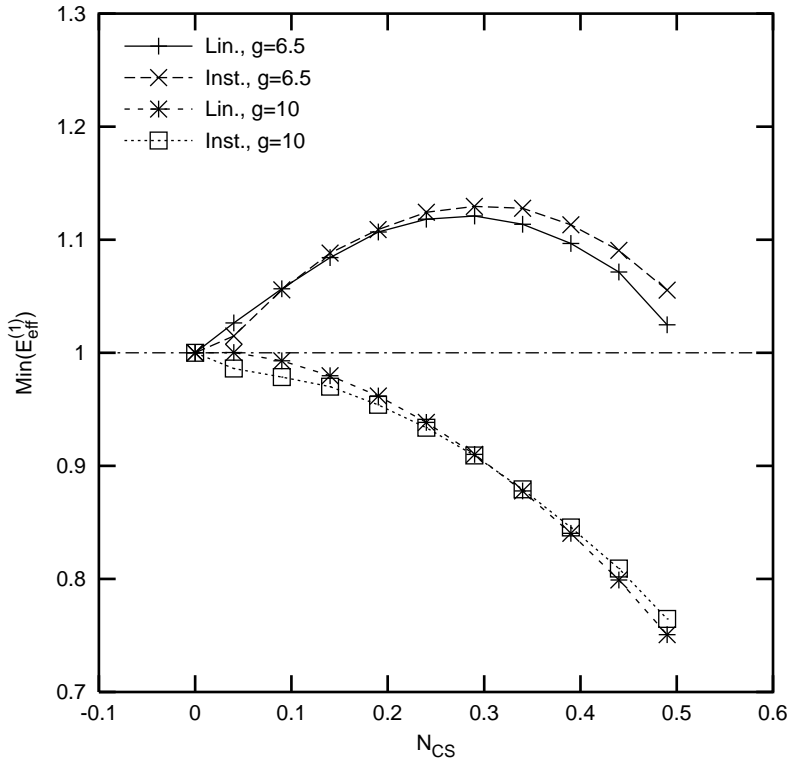


FIG. 3: Minimum  $E_{\text{eff}}^{(1)}$  (in units of  $m_f$ ) for paths from a zero-classical-energy configuration to the sphaleron. Curves denoted 'Lin.' refer to the linear path in eqs. (38, 39) while those labeled 'Inst.' are associated with the instanton path, eqs. (40,41,43).

This is the justification for considering only the linear interpolation in Fig. 2 and taking the evidence for the emergence of a new barrier and the significant energy change of the sphaleron seriously.

Note that as the gauge coupling increases, lowering the energy of the quantum-corrected sphaleron, the barrier between the fundamental fermion and the sphaleron does not persist indefinitely. We observe that for  $g = 10$ , when  $m_f$  is approximately 1.3 times our quantum-corrected sphaleron, there is no barrier and the decay mode is finally unsuppressed.

Just as in the case of the twisted-Higgs variational ansatz, in our ansätze of paths from a zero-classical-energy configuration to the sphaleron, we have not found a configuration with the associated fermion energy lower than both the perturbative fermion and the quantum-corrected sphaleron. Thus, we find no evidence for the existence of fermionic solitons in the low energy spectrum of the Standard Model within our ansätze.

## VI. CONCLUSIONS AND DISCUSSION

We have explored quantum effects of a heavy fermion on a chiral gauge theory. The quantum-corrected sphaleron is heavier than the classical sphaleron by an energy of the order of the perturbative fermion mass. This higher barrier suppresses fermion number violating processes. We also observe the creation of an energy barrier between the perturbative fermion and the sphaleron, so that a fermion with energy slightly above the sphaleron can still only decay through tunneling. This new barrier exists only for an intermediate range of perturbative fermion masses, and a heavy enough perturbative fermion is indeed unstable. We do not, however, find evidence for the existence of a soliton in the spectrum of the theory. The fermion vacuum polarization contribution seems to destabilize any would-be solitons.

It is possible that for a large enough Yukawa coupling, the Witten anomaly is saturated by states that do not have a particle interpretation. But we believe the anomaly puzzle could still be resolved by soliton states that exist outside the spherical ansatz. Although the reduced  $U(1)$  theory of the spherical ansatz reproduces the anomalous violation of fermion number, it does not have the Witten anomaly. This suggests that the ansatz might be too restrictive to resolve decoupling issues associated with the Witten anomaly. Klinkhamer has conjectured the existence of a non-spherically-symmetric sphaleron [18] derived using the same topological properties underlying the Witten anomaly, which would provide one candidate background. Like the usual sphaleron, this configuration has a zero mode because it represents the middle of a path in which a fermion level crosses zero. However, an evaluation of the stability of such a state would require a calculation of the one-loop effective energy, which is more difficult in the absence of spherical symmetry.

## ACKNOWLEDGMENTS

We would like to thank J. Goldstone, M. Quandt, and F. Wilczek for valuable discussions and also P. Sundberg for his help. E. F., R. L. J. and V. K. are supported in part by the U.S. Department of Energy (D.O.E.) under cooperative research agreement #DF-FC02-94ER40818. N. G. is supported by the U.S. Department of Energy (D.O.E.) under cooperative research agreement #DE-FG03-91ER40662 and H.W. is supported by the Deutsche Forschungsgemeinschaft under contract We 1254/3-2.

## APPENDIX A: RESULTS FROM FEYNMAN DIAGRAMS

In this Appendix we list the results from the Feynman diagram calculations mentioned in section III.

In dimensional regularization ( $d = 4 - \epsilon$ ) the counterterm coefficients, defined in eq. (12), read

$$\begin{aligned}
c_1 &= \frac{1}{6} \frac{g^2}{(4\pi)^2} \left[ \mathcal{D} - \frac{1}{2} - 3 \int_0^1 dx x(1-x) \left( 2 \ln \frac{\Delta(x, m_w^2)}{m_f^2} - x(1-x) \frac{m_w^2}{\Delta(x, m_w^2)} \right) \right], \\
c_2 &= -\frac{f^2}{(4\pi)^2} \left[ \mathcal{D} - \frac{2}{3} - 6 \int_0^1 dx x(1-x) \ln \frac{\Delta(x, m_h^2)}{m_f^2} \right], \\
c_3 &= 2m_f^2 \frac{f^2}{(4\pi)^2} (\mathcal{D} + 1), \\
c_4 &= \frac{f^4}{4(4\pi)^2} \left[ 4\mathcal{D} - \frac{m_h^2}{m_f^2} - 6 \int_0^1 dx \ln \frac{\Delta(x, m_h^2)}{m_f^2} \right]. \tag{A1}
\end{aligned}$$

We have introduced the abbreviations

$$\Delta(x, q^2) \equiv m_f^2 - x(1-x)q^2 \quad \text{and} \quad \mathcal{D} \equiv \frac{2}{\epsilon} - \gamma + \ln \frac{4\pi\mu^2}{m_f^2}, \tag{A2}$$

where  $\mu$  is the momentum scale introduced to maintain the canonical dimensions of the parameters when regularizing in fractional dimensions.

In eq. (22)  $E^{(1,2)}$  denotes the contribution to the vacuum polarization energy from first and second order renormalized Feynman diagrams. Its explicit expression reads

$$\begin{aligned}
E^{(1,2)} &= \frac{-2}{(4\pi)^2} \int \frac{d^3q}{(2\pi)^3} \left\{ f^2 \tilde{h}(\vec{q}) \tilde{h}(-\vec{q}) \left[ -(q^2 + m_h^2) + 6 \int_0^1 dx \Delta(x, -q^2) \ln \frac{\Delta(x, -q^2)}{\Delta(x, m_h^2)} \right] \right. \\
&\quad \left. - m_f^2 \tilde{p}^a(\vec{q}) \tilde{p}^a(-\vec{q}) \left[ q^2 - 6q^2 \int_0^1 dx x(1-x) \ln \frac{\Delta(x, -q^2)}{\Delta(x, m_h^2)} \right. \right. \\
&\quad \quad \left. \left. - 2m_f^2 \int_0^1 dx \ln \frac{\Delta(x, -q^2)}{m_f^2} \right] \right. \\
&\quad \left. + \frac{g^2}{2} \text{tr} \left( \vec{q} \cdot \vec{A}(\vec{q}) \vec{q} \cdot \vec{A}(-\vec{q}) \right) \left[ \frac{1}{6} - 2 \int_0^1 dx x(1-x) \ln \frac{\Delta(x, -q^2)}{\Delta(x, m_w^2)} \right. \right. \\
&\quad \quad \left. \left. - \int_0^1 dx x^2(1-x)^2 \frac{m_w^2}{\Delta(x, m_w^2)} \right] \right. \\
&\quad \left. + \frac{g^2}{2} \text{tr} \left( \vec{A}(\vec{q}) \cdot \vec{A}(-\vec{q}) \right) \left[ -\frac{q^2}{6} - \frac{2}{3} m_f^2 + 2q^2 \int_0^1 dx x(1-x) \ln \frac{\Delta(x, -q^2)}{\Delta(x, m_w^2)} \right. \right. \\
&\quad \quad \left. \left. + q^2 \int_0^1 dx x^2(1-x)^2 \frac{m_w^2}{\Delta(x, m_w^2)} + m_f^2 \int_0^1 dx \ln \frac{\Delta(x, -q^2)}{\Delta(x, m_h^2)} \right] \right\}
\end{aligned}$$



$$\begin{aligned}
& -5m_f^2 \int_0^1 dx x(1-x) \ln \frac{\Delta(x, m_h^2)}{m_f^2} \Big] \\
& -igm_f^2 \vec{q} \cdot \vec{A}(\vec{q}) \tilde{p}^a(-\vec{q}) \left[ -\frac{2}{3} + \int_0^1 dx \ln \frac{\Delta(x, -q^2)}{m_f^2} \right. \\
& \left. -6 \int_0^1 dx x(1-x) \ln \frac{\Delta(x, m_h^2)}{m_f^2} \right] \Big\}, \tag{A3}
\end{aligned}$$

with the Fourier transform of a field  $\varphi(\vec{x})$  defined in the usual way as  $\tilde{\varphi}(\vec{q}) = \int d^3x \varphi(\vec{x}) e^{i\vec{q}\cdot\vec{x}}$ . The third and fourth order counterterm contribution combined with the divergences in the third and fourth order Feynman diagrams is

$$\begin{aligned}
E^{(3,4)} = \int \frac{d^3x}{(4\pi)^2} \text{tr} \Big\{ & \frac{g^3}{6} (4i\partial_i A_j + g[A_i, A_j]) [A_j, A_i] \left[ \frac{1}{2} + 6 \int_0^1 dx x(1-x) \ln \frac{\Delta(x, m_w^2)}{m_f^2} \right. \\
& \left. -3 \int_0^1 dx x^2(1-x)^2 \frac{m_w^2}{\Delta(x, m_w^2)} \right] \\
& -g\vec{A} \cdot \left[ g\vec{A} (\phi\phi^\dagger + 2vh) + 2i (\vec{\partial}\phi) \phi^\dagger \right] \left[ -\frac{2}{3} - 6 \int_0^1 dx x(1-x) \ln \frac{\Delta(x, m_h^2)}{m_f^2} \right] \\
& \left. + f^4 (\phi\phi^\dagger + 4vh) \phi\phi^\dagger \left[ \frac{m_h^2}{4m_f^2} + \frac{3}{2} \int_0^1 dx \ln \frac{\Delta(x, m_h^2)}{m_f^2} \right] \right\}, \tag{A4}
\end{aligned}$$

where  $\phi = \Phi - v$  parameterizes the deviation of the Higgs field from its vev.

## APPENDIX B: THE DIRAC EQUATION

In this Appendix, we describe how we obtain the bound state energies of the Dirac equation and the scattering phase shifts (and their Born series) in the presence of a background potential. These quantities are required to compute the vacuum polarization energy in eq. (22).

The fermion field obeys the time-independent Dirac equation

$$H_D \Psi = \omega \Psi, \tag{B1}$$

where

$$H_D = -i\gamma^0 \gamma^i \partial_i + \gamma^0 [m_f + V(A, \Phi)], \tag{B2}$$

and  $V$  is given in eq. (6). In contrast to previous work, it is most convenient to use the chiral representation of the Dirac matrices,

$$H_D \equiv \begin{pmatrix} h_{11} & h_{12} \\ h_{21} & h_{22} \end{pmatrix} = \begin{pmatrix} i\sigma_j \partial_j + g\sigma_j A_j & m_f(s + ip\tau_j \hat{x}_j) \\ m_f(s - ip\tau_j \hat{x}_j) & -i\sigma_j \partial_j \end{pmatrix}. \tag{B3}$$

The grand spin  $\vec{G}$  is defined as the vector sum of isospin, spin and orbital angular momentum. It commutes with  $H_D$  as long as the fermion doublet is degenerate in mass and the background fields are in the spherical ansatz. We satisfy both conditions. For a given grand spin quantum number  $G$  (we suppress the grand spin projection label  $M$  throughout), the Dirac spinor  $\Psi_G$  has eight components and may be written in terms of generalized spherical harmonic functions  $\mathcal{Y}_{j,l}(\hat{x})$  with  $j = G \pm \frac{1}{2}$  and  $l = j \pm \frac{1}{2}$  as

$$\Psi_G(\vec{x}) = \begin{pmatrix} ig_1\mathcal{Y}_{G+\frac{1}{2},G+1} + g_2\mathcal{Y}_{G+\frac{1}{2},G} + g_3\mathcal{Y}_{G-\frac{1}{2},G} + ig_4\mathcal{Y}_{G-\frac{1}{2},G-1} \\ if_1\mathcal{Y}_{G+\frac{1}{2},G+1} + f_2\mathcal{Y}_{G+\frac{1}{2},G} + f_3\mathcal{Y}_{G-\frac{1}{2},G} + if_4\mathcal{Y}_{G-\frac{1}{2},G-1} \end{pmatrix}, \quad (\text{B4})$$

where  $g_i$  and  $f_i$  are radial functions and we have suppressed the grand spin labels on them. Note that in this chiral theory modes of different parity, *e.g.*  $g_1$  and  $g_2$  mix. The spherical harmonics are two-component spinors in both spin and isospin space. The special case  $\Psi_0$  is defined only in terms of  $\mathcal{Y}_{\frac{1}{2},1}$  and  $\mathcal{Y}_{\frac{1}{2},0}$  and does not contain  $g_3, g_4, f_3, f_4$ .

The matrix elements of operators like  $\tau_j \hat{x}_j$  between the spherical harmonics may be found in the literature [19]. We use them to write the Dirac equation (B2) as a set of eight coupled first-order linear differential equations in the radial functions, for fixed  $G$ . From these equations we obtain the bound state solutions ( $|\omega| < m_f$ ) in each grand spin channel using shooting algorithms. From Levinson's theorem we determine the number,  $N_G^{\text{bound}}$ , of bound states to shoot for, using phase shifts,  $\delta_G(\omega)$ , of the scattering state solutions of the Dirac equation:

$$N_G^{\text{bound}} = \frac{1}{\pi} (\delta_G(m_f) - \delta_G(\infty) + \delta_G(-m_f) - \delta_G(-\infty)). \quad (\text{B5})$$

To construct these scattering state solutions we re-write the Dirac equation as a set of second-order differential equations in the radial functions. Formally they read,

$$[h_{12}h_{21} - h_{12}(h_{22} - \omega)h_{12}^{-1}(h_{11} - \omega)] \Psi_G^U = 0, \quad (\text{B6})$$

where

$$\Psi_G^U = ig_1\mathcal{Y}_{G+\frac{1}{2},G+1} + g_2\mathcal{Y}_{G+\frac{1}{2},G} + g_3\mathcal{Y}_{G-\frac{1}{2},G} + ig_4\mathcal{Y}_{G-\frac{1}{2},G-1}$$

denotes the upper two-component spinor in  $\Psi_G$ . In the chiral representation of the Dirac matrices, we require  $s^2(r) + p^2(r) > 0$  so that  $h_{12}$  is invertible. As mentioned in section V this is a restriction on our variational ansätze. Using the known matrix elements for the

spin-isospin operators like  $\tau_i \hat{x}_i$ , we then project eq. (B6) onto grand spin channels and obtain the desired second order differential equations. They may be written in the form,

$$\sum_{j=1}^4 \left\{ D_G(r) + N_G(r) \frac{\partial}{\partial r} + M_G(r) \right\}_{ij} g_j(r) = 0, \quad (\text{B7})$$

with

$$D_G(r) = \mathbf{1} \left( \frac{\partial^2}{\partial r^2} + \frac{2}{r} \frac{\partial}{\partial r} + k^2 \right) - \frac{1}{r^2} O_G, \quad (\text{B8})$$

$$O_G = \text{diag}((G+1)(G+2), G(G+1), G(G+1), (G-1)G),$$

and  $k^2 = \omega^2 - m_f^2$ . The matrices  $N_G(r)$  and  $M_G(r)$  are given in terms of the functions  $s(r), \dots, \gamma(r)$  that specify the static background fields in the spherical ansatz, as in eq. (27). Their elements are rather lengthy and we refrain from explicitly displaying them here. As  $r \rightarrow \infty$ ,  $N_G(r) \rightarrow 0$  and  $M_G(r) \rightarrow 0$  and the differential equations decouple, as long as the potential goes to zero sufficiently fast.

We have a four-channel scattering problem. We express the four wavefunctions and four boundary conditions in matrix form,  $\mathcal{G}_{ij}(r) = g_i^{(j)}(r)$ , where the linearly independent boundary conditions are labeled by  $j = 1, 2, 3, 4$ . We then write  $\mathcal{G}(r)$  as a multiplicative modification of the matrix solution to the free differential equations,  $\mathcal{G}(r) \equiv F(r) \cdot H(kr)$ , where  $H(x) = \text{diag}(h_{G+1}^{(1)}(x), h_G^{(1)}(x), h_G^{(1)}(x), h_{G-1}^{(1)}(x))$  with  $h_\ell^{(1)}(x)$  denoting spherical Hankel functions of the first kind such that  $D_G(r) \cdot H(kr) = 0$ . (The  $4 \times 4$  matrices  $F$  and  $H$  depend on the grand spin quantum number  $G$ . For convenience we omit that label from now on.) Imposing the boundary conditions  $F(r \rightarrow \infty) = 0$  and  $F'(r \rightarrow \infty) = 0$ , it is clear that the  $i^{\text{th}}$  row of  $\mathcal{G}$  describes an outgoing spherical wave in the  $i^{\text{th}}$  channel. Similarly,  $\mathcal{G}^*$  describes incoming spherical waves. The scattering wavefunction can be written as

$$\mathcal{G}_{\text{sc}}(r) = -\mathcal{G}^*(r) + \mathcal{G}(r)S(k), \quad (\text{B9})$$

and requiring this to be regular at the origin gives the scattering matrix

$$S(k) = \lim_{r \rightarrow 0} H^{-1}(kr) F^{-1}(r) F^*(r) H^*(kr). \quad (\text{B10})$$

We are interested in the sum of the eigenphase shifts in a given grand spin channel,

$$\delta(k) = \frac{1}{2i} \text{Tr} \ln S(k) = \frac{1}{2i} \lim_{r \rightarrow 0} \text{Tr} \ln (F^{-1}(r) F^*(r)). \quad (\text{B11})$$

An efficient way to avoid any ambiguities in additive contributions of multiples of  $\pi$  in  $\delta(k)$  is to define

$$\delta(k, r) = \frac{1}{2i} \text{Tr} \ln (F^{-1}(r)F^*(r)) , \quad (\text{B12})$$

with  $\delta(k) = \delta(k, 0)$ . We then integrate

$$\frac{\partial \delta(k, r)}{\partial r} = -\Im \text{Tr} (F' F^{-1}) \quad (\text{B13})$$

along with  $F(k, r)$  from infinity to 0 with the boundary condition  $\lim_{r \rightarrow \infty} \delta(k, r) = 0$  to obtain  $\delta(k)$  as a smooth function of  $k$ . The differential equation for the matrix  $F(k, r)$ ,

$$0 = F'' + \frac{2}{r}F' + 2F'L' + \frac{1}{r^2}[F, O] + N(F' + FL') + MF , \quad (\text{B14})$$

is obtained from

$$\left[ \left\{ D(r) + N(r) \frac{\partial}{\partial r} + M(r) \right\} \mathcal{G}(r) \right] H^{-1}(kr) = 0 , \quad (\text{B15})$$

where  $L(kr) \equiv \ln H(kr)$  and primes denote derivatives with respect to the radial coordinate. The components of  $L'(kr)$  can be expressed as simple rational functions, which avoids any numerical instability that would be caused by the oscillating Hankel functions.

To construct the Born series for  $\delta(k)$ , we introduce  $F^{(n)}(k, r)$  where  $n$  labels the order in the background fields in an expansion around the zero-classical-energy configuration with  $f^{(0)}(r) = 0$  in eq. (32). We obtain the corresponding differential equations

$$\begin{aligned} 0 &= F^{(1)''} + \frac{2}{r}F^{(1)'} + 2F^{(1)'}L' + \frac{1}{r^2}[F^{(1)}, O] + N^{(1)}L' + M^{(1)} , \\ 0 &= F^{(2)''} + \frac{2}{r}F^{(2)'} + 2F^{(2)'}L' + \frac{1}{r^2}[F^{(2)}, O] + N^{(1)} \left( F^{(1)'} + F^{(1)}L' \right) \\ &\quad + N^{(2)}L' + M^{(1)}F^{(1)} + M^{(2)} , \end{aligned} \quad (\text{B16})$$

where the matrices  $N^{(i)}$  and  $M^{(i)}$  are obtained from  $N$  and  $M$  by expanding to order  $i$  in the deviation of the background fields from the above described zero-classical-energy configuration. We integrate these differential equations with the boundary conditions  $F^{(i)}(k, \infty) = 0$  and  $F^{(i)'}(k, \infty) = 0$  and obtain

$$\begin{aligned} \delta^{(1)}(k) &= -\Im \text{tr} (F^{(1)}(k, 0)) , \\ \delta^{(2)}(k) &= -\Im \text{tr} \left( F^{(2)}(k, 0) - \frac{1}{2}F^{(1)}(k, 0)^2 \right) . \end{aligned} \quad (\text{B17})$$

We eliminate the quadratic divergence from the vacuum polarization energy by subtracting these from  $\delta(k)$  and adding them back in as renormalized first and second order Feynman diagrams.

There still remains the logarithmic divergence whose elimination would require third and fourth order Born subtractions. These become considerably more complicated, so instead we use the limiting function approach as described in [12]. The idea is to subtract only the local contributions to the third and fourth Born approximants to the phase shift by identifying them with the divergent contributions to the third and fourth order Feynman diagrams. To this end we formally manipulate these divergent Feynman diagrams. To extract the local contributions we set the external momenta to zero and then integrate over the energy and the two spatial angles of the loop momenta,  $k^\mu$ , such that a (regularized) integral over  $k = |\vec{k}|$  is left. We write its integrand in the form as in eq. (22),

$$\frac{1}{2\pi} \sqrt{k^2 + m_f^2} \frac{d\delta_{\text{lim}}(k)}{dk}$$

where

$$\begin{aligned} \delta_{\text{lim}}(k) = & \frac{1}{8\pi} \left( \frac{k}{k^2 + m_f^2} + \frac{1}{m_f} \arctan \frac{m_f}{k} \right) \\ & \times \int d^3x \text{tr} \left\{ \frac{g^3}{6} (4i\partial_i A_j + g[A_i, A_j]) [A_i, A_j] - m_f^4 (\phi\phi^\dagger + 4vh) \phi\phi^\dagger \right. \\ & \left. + m_f^2 g \vec{A} \cdot [g\vec{A} (\phi\phi^\dagger + 2vh) + 2i\vec{\partial}\phi\phi^\dagger] \right\} \end{aligned} \quad (\text{B18})$$

in the  $A_0 = 0$  gauge and where  $\phi = \Phi - v$  denotes the deviation of the Higgs field from its vev.

Thus we numerically determine the bound state energies, the phase shifts, their Born series, and the limiting function. These are all ingredients in the expression for the fermion vacuum polarization energy in eq. (22).

## References

- [1] T. Appelquist and J. Carazzone, Phys. Rev. D **11** (1975) 2856.
- [2] E. D'Hoker and E. Farhi, Nucl. Phys. B **248**, 77 (1984).
- [3] E. Witten, Phys. Lett. B **117**, 324 (1982).
- [4] J. Goldstone, unpublished; E. D'Hoker and E. Farhi, Phys. Lett. B **134**, 86 (1984).
- [5] N. S. Manton, Phys. Rev. D **28**, 2019 (1983).
- [6] G. Nolte and J. Kunz, Phys. Rev. D **48**, 5905 (1993) [arXiv:hep-ph/9308290].
- [7] E. Farhi, N. Graham, P. Haagenen and R. L. Jaffe, Phys. Lett. B **427**, 334 (1998) [arXiv:hep-th/9802015].
- [8] N. Graham and R. L. Jaffe, Nucl. Phys. B **549**, 516 (1999) [arXiv:hep-th/9901023].
- [9] N. Graham, R. L. Jaffe, and H. Weigel [arXiv:hep-th/0201148] in M. Bordag, ed., *Proceedings of the Fifth Workshop on Quantum Field Theory Under the Influence of External Conditions*, Intl. J. Mod. Phys. A **17** (2002) No. 6 & 7.
- [10] B. Ratra and L. G. Yaffe, Phys. Lett. B **205**, 57 (1988).
- [11] J. Schwinger, Phys. Rev. B **94**, 1362 (1954)
- [12] E. Farhi, N. Graham, R. L. Jaffe and H. Weigel, Nucl. Phys. B **630**, 241 (2002) [arXiv:hep-th/0112217].
- [13] F. R. Klinkhamer and N. S. Manton, Phys. Rev. D **30**, 2212 (1984).
- [14] R. D. Ball, Phys. Rept. **182**, 1 (1989).
- [15] G. Ripka and S. Kahana, Phys. Rev. D **36**, 1233 (1987); J. Hartmann, F. Beck, and W. Benz, Phys. Rev. C **50**, 3088 (1994) [arXiv:hep-ph/9410263].
- [16] G. 't Hooft, Phys. Rev. D **14**, 3432 (1976) [Erratum-ibid. D **18**, 2199 (1978)].
- [17] V. Rubakov, Nucl. Phys. B **256**, 509 (1985).
- [18] F. R. Klinkhamer, Nucl. Phys. B **410**, 343 (1993) [arXiv:hep-ph/9306295].
- [19] U. Zücker, R. Alkofer, H. Reinhardt and H. Weigel, Nucl. Phys. A **570** (1994) 445 [arXiv:hep-ph/9303271].